Available online at www.sciencedirect.com
ScienceDirect
Journal of Hazardous Materials 153 (2008) 1193–1200
Journal of Hazardous Materials
www.elsevier.com/locate/jhazmat

Experimental and simulation study of hydrogen sulfide adsorption on impregnated activated carbon under anaerobic conditions

Yonghou Xiao [a,b], Shudong Wang [a], Diyong Wu [a], Quan Yuan [a,*]

[a] Dalian Institute of Chemical Physics, Chinese Academy of Sciences, Dalian Zhongshan Road 457, Dalian 116023, PR China
[b] Graduate School of the Chinese Academy of Sciences, Beijing 100039, PR China

Received 21 December 2006; received in revised form 5 April 2007; accepted 24 September 2007
Available online 29 September 2007

Abstract

In this study, a sodium carbonate impregnated activated carbon (IAC) was applied as the adsorbent for low concentration hydrogen sulfide (H_2S) in nitrogen under the anaerobic conditions in a fixed bed. The effects of impregnation, relative humidity, temperature, and the inlet H_2S concentration on the adsorption process were intensively investigated. The data of adsorption capacity were correlated by Langmuir isotherm. The results showed that the data fitted the model well within the concentration range studied. The IAC demonstrated more than three times adsorption capacity for H_2S under dry conditions, compared with the original activated carbon (AC). It was confirmed that increasing relative humidity enhanced H_2S adsorption capacity on both AC and IAC, and the adsorption capacity of H_2S decreased slightly with increasing temperature. To predict breakthrough curves, a one-dimension model for the fixed beds packed with porous adsorbents was proposed and numerically solved. Simulation results matched with the experimental data in most part of the breakthrough curves.

Keywords: Hydrogen sulfide; Impregnated activated carbon; Adsorption; Breakthrough curves; Simulation

1. Introduction

Hydrogen sulfide (H_2S) is one of the common malodorous compounds that can be found in volcanic gases, petroleum deposits, natural gas, and emissions from many industrial plants [1]. This harmful gas can cause health problems to human, and even as low as 1 part per million (ppm) of H_2S has detrimental effects on the catalysts [2]. Therefore, removing H_2S from gases is of significance in both life and industry.

Among the various methods used to remove low concentration H_2S from gases, adsorption–catalysis by activated carbons (AC) is considered as an efficient and economical approach [3–15]. The uniqueness of activated carbons as adsorbents and catalyst supports is related to their high surface area, developed pore volume, surface properties, and possibility of modification. Moreover, activated carbons are relatively inexpensive materials as compared to many other inorganic adsorbents such as zeolites, alumina, and silica. Although activated carbon works well for removal of low concentration H_2S, impregnated activated carbon is a better choice for more effective removal [16–27].

Good performance for H_2S removal can be obtained by impregnating with caustic materials such as NaOH or KOH [17–25], and it makes only a slight increase in the cost of materials. Other materials, such as KI, $KMnO_4$, K_2CO_3 and Na_2CO_3, are also used as impregnates for gas desulphurization [16–18]. It has been reported that the total removal capacity could be increased as much as about 40–60 times that of the original carbons, by impregnating with Na_2CO_3 [17,22]. The technology based on H_2S selective oxidation by air to elemental sulfur and water via the following reaction (I) gains public acceptance as an "environment-friendly" process to reduce secondary pollution for several reasons.

$$H_2S + \frac{1}{2}\frac{1}{O_2} \rightarrow \frac{1}{n}S_n + H_2O \quad \text{(I)}$$

First, the reaction has the thermodynamic potential to remove H_2S to the part per billion (ppb) levels. Second, the gases are purified and element sulfur or sulfate is stored in a single-step process at ambient temperatures. Third, the presence of steam promotes the conversion of H_2S on activated carbon,

* Corresponding author. Tel.: +86 411 84687994; fax: +86 411 84662365.
E-mail address: qyuan@dicp.ac.cn (Q. Yuan).

0304-3894/$ – see front matter © 2007 Elsevier B.V. All rights reserved.
doi:10.1016/j.jhazmat.2007.09.081

Nomenclature

C	bulk concentration of H_2S in column (mol/m^3)
C_0	inlet (feed) concentration of H_2S (mol/m^3)
C_t	outlet concentration of H_2S (mol/m^3)
$C_{t,e}$	equilibrium concentration of H_2S (mol/m^3)
C_{out}^{cal}	calculated outlet concentration of H_2S (mol/m^3)
C_{out}^{exp}	experimental outlet concentration of H_2S (mol/m^3)
C_p	concentration of H_2S in pores (mol/m^3)
d_p	diameter of the particle (m)
D_{ep}	effective intraparticle coefficient (m^2/s)
D_L	axial dispersion coefficient (m^2/s)
D_m	dispersion coefficient (m^2/s)
k_f	external film mass transfer coefficient (m/s)
K_L	Langmuir adsorption constant (m^3/ mol)
L	length of the adsorption column (m)
m_s	the mass of the adsorbent (g)
M	molecular mass
P_{bar}	pressure (Pa)
q	adsorbed H_2S concentration in the column (mg H_2S/g adsorbent)
q_m	maximum adsorption capacity of H_2S (mg H_2S/g adsorbent)
Q	flow rate (m^3/min)
r	radial distance of adsorbent (m)
R_p	radius of adsorbent core (m)
Sc	Schmidt number
Sh	Sherwood number relative to particle
t	time (min)
t_e	equilibrium time (min)
T	temperature (K)
u	interstitial fluid velocity along the column (m/s)
Z	the position along the bed (m)

Greek letters

ε_b	bed voidage
ε_p	particle porosity
ρ_p	skeletal particle density (kg/m^3)
ρ_T	true particle density (kg/m^3)
ρ	gas density (kg/m^3)
μ	dynamic viscosity

whereas steam actually inhibits the capture of H_2S with ZnO [28].

Adsorption/oxidation by Na_2CO_3 impregnated activated carbon (IAC) was widely studied as a promising method to control pollution of H_2S. However, the role of Na_2CO_3 and water in the process is still not clearly understood. Additionally, it is widely accepted that pore diffusion process governs the adsorption rate [29,30], at which gas-phase species reach the activated carbon surface. Previous researchers [31,32] have intensively investigated the experiments and modeling of VOCs dynamic adsorption onto activated carbon. However, there are only a few studies focused on modeling of H_2S adsorption process [33].

Table 1
Characteristics of the adsorbents

Parameters	AC	IAC
BET surface area (m^2/g)	732	715
Total pore volume (mL/g)	0.416	0.406
Micropore volume (mL/g)	0.226	0.218
Apparent density (g/mL)	0.427	0.451
Real density (g/mL)	1.80	1.84

The objective of this study is to investigate the process of H_2S adsorption onto IAC. The promotion of impregnation by Na_2CO_3 for H_2S adsorption on AC is investigated under anoxic conditions in a fixed bed. The effects of the operating variables on the process are also studied. Furthermore, Langmuir isotherm is used to fit the adsorption data. To predict breakthrough curves, a one-dimension model, which accounts for nonlinear adsorption systems in a fixed bed packed with porous adsorbents coupled with axial dispersion, film mass transfer and intraparticle mass transfer, is developed and numerically solved.

2. Materials and methods

2.1. Materials

The carbons used in the test are commercial coal based granular activated carbons (GAC). The carbons were impregnated according to the following procedure. First, impregnation was done by mixing 50 g of carbon with 25 mL of 6% Na_2CO_3 solution for 30 min. Then the samples were taken out from the mother solution and dried at 120 °C to evaporate water for 10 h before use. The impregnated activated carbons and the original one are referred to IAC and AC, respectively. The characteristics of the adsorbents are summarized in Table 1.

2.2. Experimental apparatus

A schematic flow diagram of the adsorption process is illustrated in Fig. 1. The apparatus consists of a stainless steel column (8 mm in i.d., 200 mm in length) immersed in a thermostatic

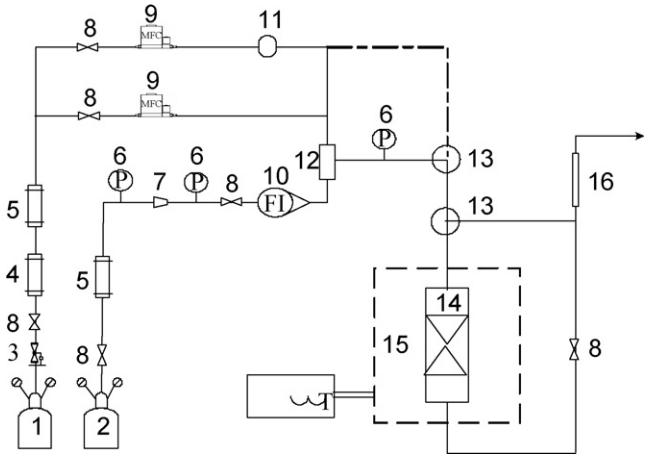

Fig. 1. Schematic diagram of experimental apparatus.

bath, which was used to provide a uniform and constant temperature. Mixtures of the gases were prepared in a mixer and mass flow controllers were used to regulate the gas flow rates. The adsorption column was also used to dehumidify the adsorbents in nitrogen flow. An externally heating furnace was used to keep constant temperature for the dehumidification process. Different relative humidity was regulated by choosing a saturation temperature, which gave the desired water vapor pressure, and the carrier gas (N_2) passed the bubbler in a specified flow rate.

2.3. Evaluation of H_2S adsorption capacity

Dynamic adsorption tests were carried out to evaluate the adsorption capacity of H_2S on AC and IAC. In a typical run, ca. 1.5 g of the adsorbent sample (450–500 μm sieve fractions) was carefully packed into the adsorption column. The adsorbents were heated to remove water for ca. 10 h under the nitrogen atmosphere at 260 °C for the test performed under dry conditions. Then adsorption behavior of H_2S was tested. The mixed gases containing 100–1000 ppm of H_2S passed through the adsorbent bed at a flowrate of about 120 mL/min. The adsorption column was kept at either 30 or 60 °C in the adsorption process.

The concentration of H_2S was measured by sulfur Microcoulomb Analyzer and Varian 3800 gas chromatograph with a pulsed flame photometric detector permitting the detection levels as low as 0.5 ppm. The test was stopped at the point that the elution concentration is approximately equal to the inlet concentration, and it does not change with time any more. To such time the adsorption gets the equilibrium state.

Then adsorption capacity q_m was calculated by integrating the area above the breakthrough curve for a given inlet H_2S concentration, mass of adsorbents and flow rate, as it is defined by Eq. (1).

$$q_m = \frac{34C_0Q}{1000m_S}\int_0^{t_e}\left(1-\frac{C_t}{C_0}\right)\mathrm{d}t \tag{1}$$

3. Theory and calculation

A porous particle diffusion model, which involves the material balance equations in both of the gas-phase and the pore-phase, was proposed to simulate the adsorption process [29]. The following assumptions were made to construct the model equations:

(1) The process operates under isothermal conditions.
(2) Axial dispersion is considered to account for non-ideal flux along the longitudinal axis of the column, and there is no radial concentration gradient in the column.
(3) The adsorbent particles are spherical and homogeneous in size and density.
(4) The linear velocity of the gas-phase along the column, and the mass transfer parameters are independent of the concentration in the bulk gas phase.
(5) Mass transfer across the boundary layer surrounding the solid particles is characterized by the external film mass transfer coefficient, k_f.
(6) Intraparticle mass transport is characterized by the effective pore diffusion coefficient, D_{ep}, and surface diffusion is neglected.
(7) There is a local equilibrium between the gas concentration adsorbed on the solid and that of the local.

3.1. Mathematical model

Based on the above assumption, for a control volume dZ the mass balance for the bed can be expressed as:

$$\partial C/\partial t = D_L\partial^2 C/\partial Z^2 - u\partial C/\partial Z - 3k_f/R_p(1-\varepsilon_b)/\varepsilon_b\partial q/\partial t \tag{2}$$

The boundary conditions at both ends of the column are given as following:

$$\frac{-D_L\partial C}{\partial Z}|_{Z=0} = u(C_0 - C|_{Z=0}) \tag{3}$$

$$\frac{\partial C}{\partial Z}|_{Z=L} = 0 \tag{4}$$

The mass balance within a differential radial section of an adsorbent particle can be expressed as:

$$\partial C/\partial t + (1-\varepsilon_p)/\varepsilon_p\rho_T\,\partial q/\partial t = D_{ep}(\partial^2 C/\partial r^2 + 2/r\,\partial C/\partial r) \tag{5}$$

Let:

$$\partial q/\partial t = \partial C_P/\partial t\,\partial q/\partial C_p \tag{6}$$

Then, Eq. (5) becomes:

$$\partial C_p/\partial t = 1/[1+\rho_T(1-\varepsilon_p/\varepsilon_p)\partial q/\partial C_p]D_{ep}(\partial^2 C_p/\partial r^2 + 2/r\partial C_p/\partial r) \tag{7}$$

The symmetry condition at the center of the particles is as following:

$$\frac{\partial C_p}{\partial r}|_{r=0} = 0 \tag{8}$$

The continuity condition on the external surface of the adsorbent particles is given as:

$$\frac{D_{ep}\varepsilon_p\partial C_p}{\partial r}|_{r=R_p} = k_f(C - C_p|_{r=R_p}) \tag{9}$$

Finally, the following initial conditions are considered

$$\begin{aligned} &C = 0, && 0 \le Z \le L && (t \le 0)\\ &C = C_0, && Z = 0 && (t > 0)\\ &C_p = 0, && 0 \le Z \le L && (t \le 0)\\ &q = 0, && 0 \le Z \le L && (t \le 0) \end{aligned} \tag{10}$$

3.2. Breakthrough curves and equilibrium isotherm

Breakthrough curves can show the loading behavior of H_2S removal from the bulk gas-phase in a fixed bed. Dimensionless outlet concentration is defined as the ratio of effluent concentration to inlet concentration (C_t/C_0), as a function of time for a given bed height.

Solid phase concentration, q, is related to pore-phase concentration C_p by isotherms. The nonlinear Langmuir isotherm was used to represent the q and C_p relationship in the concentration range studied.

The Langmuir isotherm [34] has the general form:

$$q = \frac{q_m K_L C_p}{1 + K_L C_p} \tag{11}$$

where q_m is the adsorption capacity (mg/g AC) and K_L (m^3/mg) is related to the energy of adsorption.

3.3. Axial dispersion

Axial dispersion coefficient, D_L, is estimated by the Wakao–Funazkri correlation [35]:

$$\frac{\varepsilon_b D_L}{D_m} = 20 + 0.5 Sc\, Re \tag{12}$$

The Reynolds number, Re, and the Schmidt number, Sc, in Eq. (12) are defined as:

$$Re = \frac{d_p u \rho}{\mu} \tag{13}$$

$$Sc = \frac{\mu}{\rho D_m} \tag{14}$$

And the molecular diffusion coefficient [36] is defined as:

$$Dm = \frac{0.00143 T^{1.75}}{10000 P_{bar} M_{AB}^{0.5} (V_{N_2}^{1/3} + V_{H_2S}^{1/3})^2} \tag{15}$$

3.4. Film diffusion

The Wilson and Geankoplis correlation [29] were used to determine the film mass transfer coefficient, k_f, in the low Reynolds number range:

$$Sh = \frac{2 k_f R_P}{D_m} = \frac{1.09}{\varepsilon_b \mathrm{Re}^{0.33} Sc^{0.33}} \tag{16}$$

Re and Sc, are defined by (13) and (14), respectively.

Method of line (MOL) was applied to numerically solve the Eqs. (2) and (7). The finite volume method was applied to discretize the space variables Z and r of the partial differential Eqs. (2) and (7), then the resulting ODEs were integrated using Gear's method.

The value of D_{ep} was obtained by fitting the mathematical model to the experimental breakthrough curves and further optimized using the BFGS method. The objective function was defined as:

$$\phi = \sum_{i=1}^{N} [(C_{out}^{exp} - C_{out}^{cal})^2] \tag{17}$$

Table 2
The Langmuir isotherm parameters obtained by using linear method under dry conditions

Adsorbents	AC		IAC	
Temperature (°C)	30	60	30	60
q_m (mg/g)	2.7	2.6	9.4	9.3
K_L (m^3/mg)	0.014	0.012	0.018	0.0062
R^2	0.99	0.97	0.98	0.99

4. Results and discussion

4.1. Adsorption equilibrium study

The equilibrium adsorption capacity of H_2S on AC and IAC obtained from the dynamic adsorption was attempted to fit by Langmuir isotherm, and the parameters were listed in Table 2. Fig. 2 shows the H_2S adsorption equilibrium curves on AC and IAC under dry conditions at 30 and 60 °C. It is demonstrated that the equilibriums were favorable and nonlinear for both of the AC-H_2S and IAC-H_2S systems. Langmuir isotherm adequately described it within the temperature and the concentration range reported.

4.2. Effect of impregnation

To reveal the promotion of impregnation with Na_2CO_3 for H_2S adsorption on activated carbons, dynamic adsorption tests were performed. The breakthrough curves were measured under dry conditions and shown in Fig. 3. The results clearly indicated that the removal rate was substantially boosted and the breakthrough was delayed by impregnation.

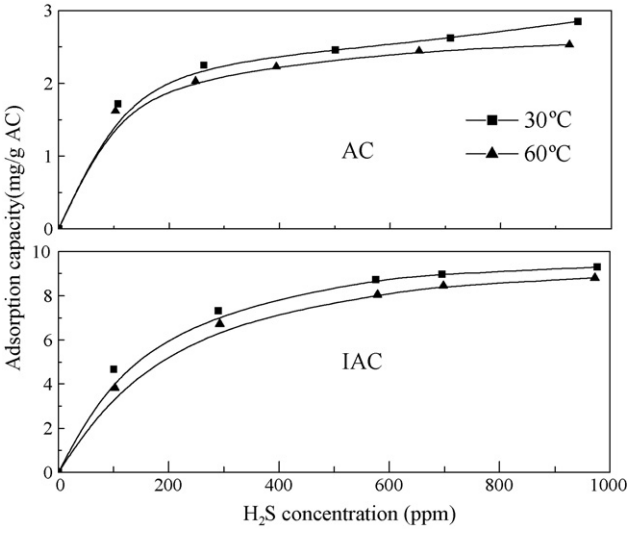

Fig. 2. Effect of impregnation with Na_2CO_3 on H_2S adsorption capacities on AC (temperature: 30 and 60 °C; under dry conditions).

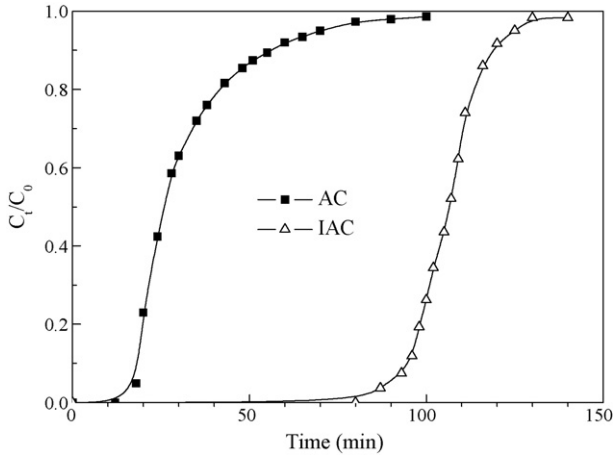

Fig. 3. Effect of impregnation with Na_2CO_3 on the breakthrough curves of H_2S adsorption on AC (temperature: 30 °C; H_2S concentration: ca. 700 ppm; under dry conditions).

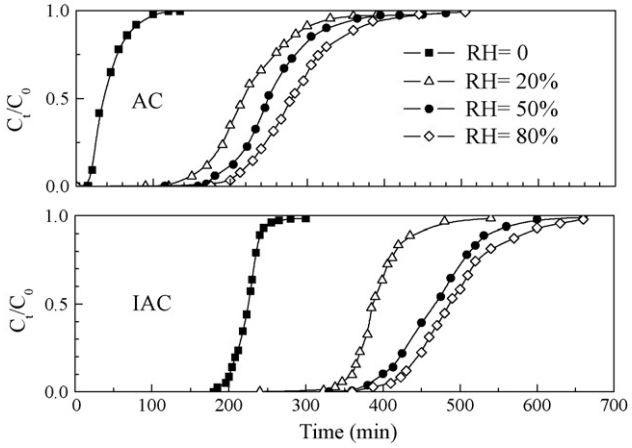

Fig. 4. Effect of relative humidity on the breakthrough curves of H_2S adsorption on AC and IAC (temperature: 30 °C; H_2S concentration: ca. 200 ppm).

As presented in Fig. 2, the equilibrium sorption capacity of H_2S increased more than three times after impregnation, though the BET surface area, micropore volume of the activated carbon was reduced slightly. The impregnant might occupy a portion of the carbon pore volume and surface area, thus limiting physical adsorption. Nevertheless, the sorption capacity on the impregnated carbons is much greater than that of the unmodified carbon. The results confirm that after impregnation, H_2S is no longer removed mainly by physical adsorption but chemical reaction [18]. The impregnated Na_2CO_3 changes the surface properties and enforces the interactions between activated carbons and H_2S molecules. When the molecules of H_2S contact the impregnating compound (Na_2CO_3), they react instantaneously.

As illustrated in Table 3, it is nearly 1 mol H_2S per mol Na_2CO_3 that the difference of the equilibrium adsorption capacity for H_2S on AC and IAC; therefore, reaction (II) was the major reaction scheme, which was able to explain the behavior of chemical reaction part for H_2S adsorption by IAC. When the system is in absence of oxygen, the capacity is limited, and the reaction occurs until most of the Na_2CO_3 is consumed. Previous researchers [25] have reported the similar results for the caustic-impregnated activated carbon. The stoichiometric ratio between the impregnant and H_2S approximately equals to one.

$$H_2S(g) + Na_2CO_3(s) \rightarrow NaHS + NaHCO_3 \quad \text{(II)}$$

Table 3
Comparison of the adsorption capacities of H_2S on AC and IAC at 30 °C, under dry conditions

	H_2S concentration (ppm)				
	200	400	600	800	1000
Sorption capacity of AC (mg/g)	2.1	2.6	2.5	2.7	3.0
Sorption capacity of IAC (mg/g)	7.7	8.7	8.6	9.0	9.3
Difference of AC and IAC (mg/g)	5.6	6.1	6.1	6.3	6.3

4.3. Effect of relative humidity

Experiments were carried out to investigate the effect of relative humidity (RH) on the performance of H_2S dynamic adsorption on AC and IAC. The relative humidity was varied from 0 to 80% at the temperature of 30 °C. The dramatic effect of water on H_2S adsorption is shown in Fig. 4, which indicates the comparison of the breakthrough curves of H_2S adsorption on AC and IAC with increasing relative humidity. Under dry conditions, a rapid breakthrough was observed and the outlet concentration increased rapidly. It can also be seen that the time for breakthrough was delayed by increasing relative humidity. It confirms that water plays a key role in the H_2S uptake process [10–18]. When humidity is high, a sufficient amount of water is adsorbed and capillary condensation of water vapor takes place in the pores of activated carbons. A water film is thus formed on the internal surface of AC. It was proposed that the molecules of H_2S was transported and dissolved to produce H^+ and HS^- ions into the water film. Therefore, presence of water has a beneficial effect on the adsorption performance of H_2S on AC and IAC.

The adsorption isotherms of H_2S on AC and IAC under different relative humidity at 30 °C are showed in Fig. 5. The data

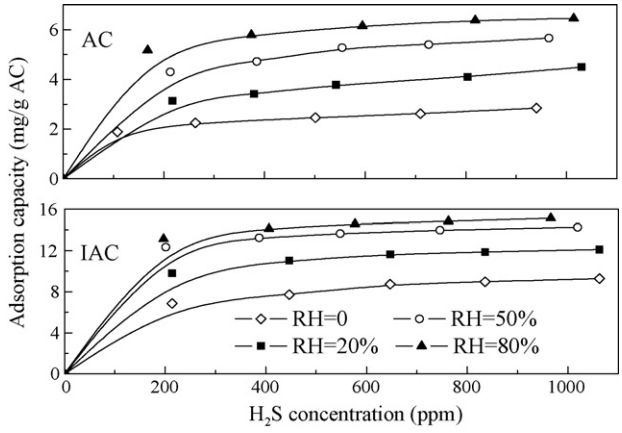

Fig. 5. Effect of relative humidity on H_2S adsorption capacities on AC and IAC (temperature: 30 °C).

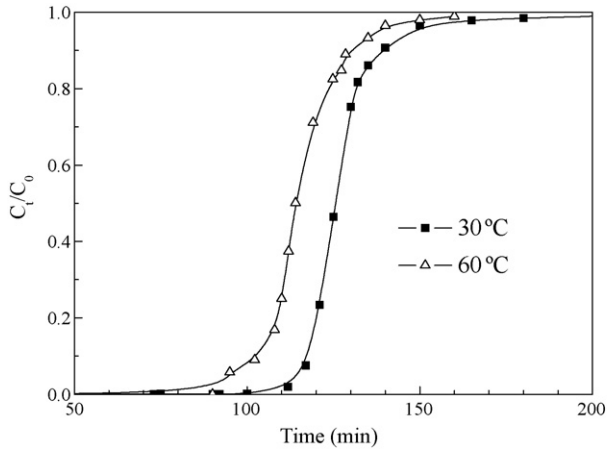

Fig. 6. Effect of temperature on the breakthrough curves of H_2S adsorption on IAC (H_2S concentration: 580 ppm; under dry conditions).

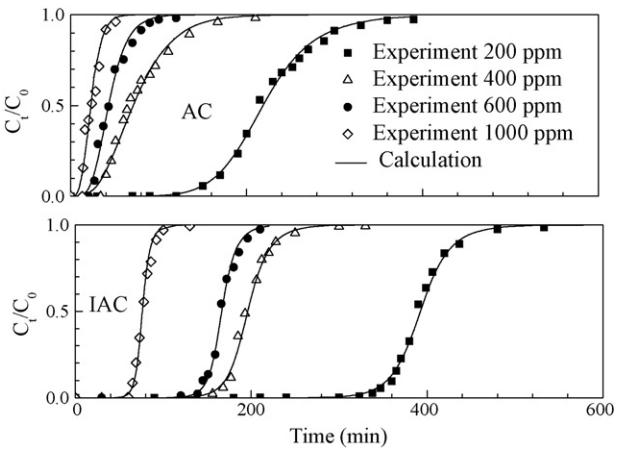

Fig. 7. Simulated (lines) and experimental (points) breakthrough curves of different concentration H_2S adsorption on AC and IAC (temperature: 30 °C; RH: 20%).

clearly show that with relative humidity increasing, the adsorption capacity of H_2S on AC and IAC increased significantly. In addition, the IAC has a higher efficiency for H_2S adsorption, in comparison with AC under different relative humidity. These results support the hypothesis of that a basic environment is critical for dissolving and reaction of H_2S [3–6,25,26], which is provided by the impregnation of Na_2CO_3 in this study. By increasing the pH value of the carbon surface, Na_2CO_3 causes an increase in the HS^- ion concentration. And it was well known that Na_2CO_3 was a strong moisture absorber when it existed in the pores and surface of activated carbon the water film might be produced easily onto the surface of the IAC to absorb H_2S.

4.4. Effect of temperature

Apart from relative humidity, temperature may also be an important factor, which can influence the adsorption processes. The effect of temperature on the performance of H_2S adsorption on IAC under dry condition is shown in Fig. 6. With increase in temperature the breakthrough was achieved faster and equilibrium adsorption capacity decreased slightly. Because adsorption is a slightly exothermal process, higher temperature will probably enhance chemisorptions but has disadvantage on the physical adsorption. Thus, an increase in the operating temperature caused lower values of the maximum capacity of the adsorbent q_m.

4.5. Effect of inlet H_2S concentration

To study the effect of the initial H_2S concentration on the adsorption process, several experiments were performed. The breakthrough curves for H_2S adsorption on AC and IAC are presented in Fig. 7. The effect of inlet H_2S concentration on the dynamic adsorption process was significant, on the both samples. The sorption capacity increased when the inlet H_2S concentration increased. For lower feed concentrations, the lower mass-transfer flux was achieved from the bulk gas to the particle surface, due to the decreased driving force. On the other hand, higher feed concentration yields enhanced driving force along the pores, thus resulting in the steeper breakthrough curves and the faster equilibrium. Furthermore, increasing inlet H_2S concentration at specific flow rate causes a shorter breakthrough time. It is well established that a given mass of adsorbents can only adsorb a fixed amount of H_2S under certain conditions; therefore, the adsorbents are saturated more quickly under high concentration.

4.6. Simulation study

The one-dimension diffusion model was developed to simulate the performance of H_2S dynamic adsorption on AC and IAC. The effective diffusivities of H_2S were obtained by using the calculated breakthrough curves to fit the experimental ones. And the results are shown in Table 4. Moreover, they were used to predict the breakthrough curves at some other operation conditions.

Fig. 8 shows the comparison of the breakthrough curves of H_2S adsorption on IAC, which included experimental results and simulation for different inlet concentrations. The experimental and the calculated results appeared to be in good agreement for most part of the initial zone of the breakthrough curves, but deviated marginally in the tailing zone. And at the end of the breakthrough curves, a small slope was shown, indicating that adsorption rate became very small when adsorbent approached to equilibrium.

Based on the above results, the adsorption mechanism of H_2S on AC and IAC was proposed as follows. Gaseous molecules of H_2S diffuse into the AC and IAC particles through the macropores first, due to the concentration gradient in the gas phase.

Table 4
Effective diffusivity (m^2/s) of H_2S sorption on AC and IAC at 30 °C, under dry conditions

Adsorbents	Concentration (ppm)			
	200	400	600	1000
AC	1.59×10^{-6}	1.68×10^{-6}	1.75×10^{-6}	2.01×10^{-6}
IAC	1.66×10^{-6}	1.72×10^{-6}	1.81×10^{-6}	2.10×10^{-6}

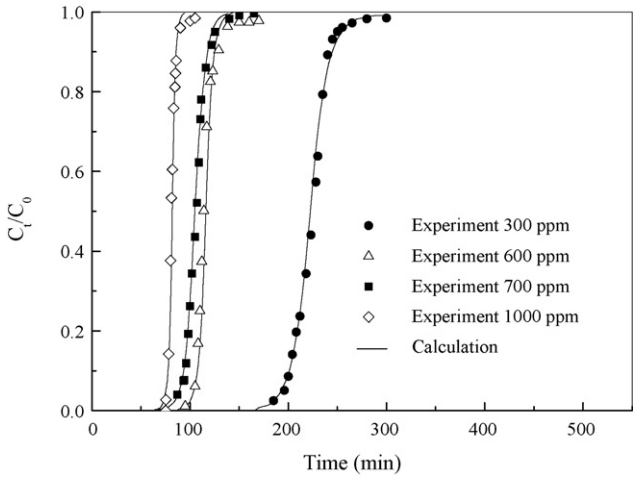

Fig. 8. Comparison of breakthrough curves of different concentration H_2S adsorption on IAC between experiment results (dots) and model (solid line) (temperature: 30 °C; under dry conditions).

Once the gas molecules contact Na_2CO_3 on the wall of macropores, they react instantaneously and irreversibly. That is to say, both the reaction and the adsorption rates are much faster than that of the intraparticle diffusion for this system. This result was in agreement with that was reported by Ikeda et al [22]. The adsorption process is likely governed by the intraparticle diffusion [29,30].

5. Conclusions

The results obtained from H_2S adsorption on AC and IAC in fixed bed demonstrates that impregnation with Na_2CO_3 increases the adsorption capacity under anaerobic conditions. The impregnation changes the surface properties and enforces the interactions between activated carbon and H_2S molecules. The adsorption equilibrium is favorable and nonlinear for both AC-H_2S and IAC-H_2S systems and it can be adequately described by Langmuir isotherm. When the relative humidity increases, the H_2S adsorption capacity is significantly enhanced on either AC or IAC and the breakthrough time is delayed. The adsorption capacities of H_2S on IAC decrease slightly with temperature increasing. Moreover, the one-dimension diffusion model can well predict the H_2S dynamic adsorption behavior. The process of H_2S adsorption on AC and IAC is likely governed by the intraparticle diffusion.

Acknowledgements

This study was financially supported by the National Natural Science Foundation of China grant No. 20476103. The help of Dr. Li Wang in performing experiments is appreciated. The authors would like to thank the anonymous reviewers for their insightful suggestions.

References

[1] G. Busca, C. Pistarino, Technologies for the abatement of sulphide compounds from gaseous streams: a comparative overview, J. Loss Prevent. Proc. 16 (2003) 363–371.
[2] P. Forzatti, L. Lietti, Catalyst deactivation, Catal. Today 52 (1999) 165–181.
[3] A. Bagreev, F. Adib, T.J. Bandosz, pH of activated carbon surface as an indication of its suitability for H_2S removal from moist air streams, Carbon 39 (2001) 1897–1905.
[4] F. Adib, A. Bagreev, T.J. Bandosz, Effect of pH and surface chemistry on the mechanism of H_2S removal by activated carbons, J. Colloid Interf. Sci. 216 (1999) 360–369.
[5] F. Adib, A. Bagreev, T.J. Bandosz, Effect of surface characteristics of wood-based activated carbons on adsorption of hydrogen sulfide, J. Colloid Interf. Sci. 214 (1999) 407–415.
[6] F. Adib, A. Bagreev, T.J. Bandosz, On the possibility of water regeneration of unimpregnated activated carbons used as hydrogen sulfide adsorbents, Ind. Eng. Chem. Res. 39 (2000) 2439–2446.
[7] J. Masuda, J. Fukuyama, S. Fujii, Influence of concurrent substances on removal of hydrogen sulfide by activated carbon, Chemosphere 39 (1999) 1611–1616.
[8] A.K. Dalai, A. Majumdar, E.L. Tollefson, Low temperature catalytic oxidation of hydrogen sulfide in sour produced waste water using activated carbon catalysts, Environ. Sci. Technol. 33 (1999) 2241–2246.
[9] T.J. Bandosz, A. Bagreev, F. Adib, A. Turk, Unmodified versus caustics-impregnated carbons for control of hydrogen sulfide emissions from sewage treatment plants, Environ. Sci. Technol. 34 (2000) 1069–1074.
[10] T.J. Bandosz, Effect of pore structure and surface chemistry of virgin activated carbons on removal of hydrogen sulfide, Carbon 37 (1999) 483–491.
[11] J. Klein, L.-D. Henning, Catalytic oxidation of hydrogen sulfide on activated carbons, Fuel 63 (1984) 1064–1067.
[12] V. Meeyoo, D.L. Trimm, N.W. Cant, Adsorption–reaction processes for the removal of hydrogen sulphide from gas streams, J. Chem. Tech. Biotech. 68 (1997) 411–416.
[13] V. Meeyoo, J.H. Lee, D.L. Trimm, Hydrogen sulfide emission control by combined adsorption and catalytic combustion, Catal. Today 44 (1998) 67–72.
[14] A. Bagreev, T.J. Bandosz, H_2S adsorption/oxidation on unmodified activated carbons: importance of prehumidification, Carbon 39 (2001) 2303–2311.
[15] A. Primavera, A. Trovarelli, P. Andreussi, G. Dolcetti, The effect of water in the low-temperature catalytic oxidation of hydrogen sulfide to sulfur over activated carbon, Appl. Catal. A 173 (1998) 185–192.
[16] K.D. Henning, S. Schafer, Impregnated activated carbon for environmental protection, Gas Sep. Purif. 7 (1993) 235–240.
[17] X.Y. Tan, The Process to remove H_2S on impregnated activated carbon, PhD thesis, Dalian Institute of Chemical Physics, Chinese Academy of Sciences, 1999.
[18] H.L. Chiang, J.H. Tsai, C.L. Tsai, Y.C. Hsu, Adsorption characteristics of alkaline activated carbon exemplified by water vapor, H_2S, and CH_3SH gas, Sep. Sci. Technol. 35 (2000) 903–918.
[19] A. Turk, K. Mahmood, J. Mozaffari, Activated carbon for air purification in NEW-YORK-CITY sewage-treatment plants, Water Sci. Technol. 27 (1993) 121–126.
[20] H.L. Chiang, J.H. Tsai, G.M. Chang, Y.C. Hsu, Adsorption kinetic characteristics of H_2S on activated carbon, Adsorption 8 (2002) 325–340.
[21] J.H. Tsai, F.T. Jeng, H.L. Chiang, Removal of H_2S from exhaust gas by use of alkaline activated carbon, Adsorption 7 (2001) 357–366.
[22] H. Ikeda, H. Asaba, Y. Ikeda, Removal of H_2S, CH_3SH and $(CH_3)_3N$ from air by use of chemically treated activated carbon, J. Chem. Eng. Jpn. 21 (1983) 91–97.
[23] R. Yan, D.T. Liang, L. Tsen, J.H. Tay, Kinetics and mechanisms of H_2S adsorption by alkaline activated carbon, Environ. Sci. Technol. 36 (2002) 4460–4466.
[24] R. Yan, T. Chin, Y.L. Ng, H. Duan, D.T. Liang, J.H. Tay, Influence of surface properties on the mechanism of H_2S removal by alkaline activated carbons, Environ. Sci. Technol. 38 (2004) 316–323.
[25] A. Bagreev, T.J. Bandosz, A role of sodium hydroxide in the process of hydrogen sulfide adsorption/oxidation on caustic-impregnated activated carbons, Ind. Eng. Chem. Res. 41 (2002) 672–679.
[26] L. Meljac, L. Perier-camby, G. Thomas, Creation of active sites by impregnation of carbon fibers: application to the fixation of hydrogen sulfide, J. Colloid Interf. Sci. 274 (2004) 133–141.

[27] A. Bagreev, J.A. Menendez, I. Dukhno, Y. Tarasenko, Bituminous coal-based activated carbons modified with nitrogen as adsorbents of hydrogen sulfide, Carbon 42 (2004) 469–476.
[28] I.I. Novochinskii, C. Song, X. Ma, X. Liu, L. Shore, J. Lampert, R.J. Farrauto, Low-Temperature H_2S removal from steam-containing gas mixtures with ZnO for fuel cell application. 1. ZnO particles and extrudates, Energy Fuels 18 (2004) 576–583.
[29] R.T. Yang, Gas Separation by Adsorption Processes, Butterworth, Boston, 1987.
[30] D.M. Ruthven, Principles of Adsorption and Adsorption Processes, Wiley, New York, NY, 1984.
[31] T. Murillo, E. Garcia, M.S. Aylon, Adsorption of phenanthrene on activated carbons: Breakthrough curve modeling, Carbon 42 (2004) 2009–2017.
[32] C.L. Chuang, P.C. Chiang, E.E. Chang, Modeling, VOCs adsorption onto activated carbon, Chemosphere 53 (2003) 17–27.
[33] H.L. Chiang, J.H. Tsai, D.H. Chang, F.T. Jeng, Diffusion of hydrogen sulfide and methyl mercaptan onto microporous alkaline activated carbon, Chemosphere 41 (2000) 1227–1232.
[34] W.J. Weber Jr., Physicochemical Processes for Water Quality Control, John Wiley & Sons Inc., New York, 1972, pp. 199–228.
[35] N. Wakao, T. Funazkri, Effect of fluid dispersion coefficients on particle-to-fluid mass transfer coefficients in packed beds: Correlation of Sherwood numbers, Chem. Eng. Sci. 33 (1978) 1375–1384.
[36] E.N. Fuller, P.D. Schettler, J.C. Giddings, A new method for prediction of binary gas-phase diffusion coefficients, Ind. Eng. Chem. 58 (1966) 18–27.